Lab on a Chip

Miniaturisation for chemistry, biology & bioengineering

www.rsc.org/loc

Volume 8 | Number 11 | November 2008 | Pages 1753–1964

ISSN 1473-0197

RSC Publishing

Using ratchets and sorters to fractionate motile cells of *Escherichia coli* by length

S. Elizabeth Hulme,[a] Willow R. DiLuzio,[a,b] Sergey S. Shevkoplyas,[a] Linda Turner,[c] Michael Mayer,[a] Howard C. Berg[c] and George M. Whitesides*[a]

Received 11th June 2008, Accepted 21st August 2008
First published as an Advance Article on the web 1st October 2008
DOI: 10.1039/b809892a

This paper describes the fabrication of a composite agar/PDMS device for enriching short cells in a population of motile *Escherichia coli.* The device incorporated ratcheting microchannels, which directed the motion of swimming cells of *E. coli* through the device, and three sorting junctions, which isolated successively shorter populations of bacteria. The ratcheting microchannels guided cells through the device with an average rate of displacement of (32 ± 9) μm s^{-1}. Within the device, the average length of the cells decreased from 3.8 μm (Coefficient of Variation, CV: 21%) at the entrance, to 3.4 μm (CV: 16%) after the first sorting junction, to 3.2 μm (CV: 19%) after the second sorting junction, to 3.0 μm (CV: 19%) after the third sorting junction.

Introduction

This paper describes a microfabricated device that makes it possible to separate motile cells of *Escherichia coli* by length. The device has two principal components: (i) ratcheting microchannels, which guide cells unidirectionally through the device, and (ii) sorting junctions, which use the turning radius of swimming cells in a microfluidic channel to separate short cells from the population. We believe this ability to isolate the shortest cells in a population will be useful for producing synchronized populations of bacteria. The device consisted of a thin film (1 mm in thickness) of poly(dimethyl siloxane) (PDMS) embossed with microchannels—fabricated using soft lithography[1]—in conformal contact with an agar surface;[2] channels in the device therefore had a floor of agar and a ceiling and sidewalls of PDMS. The operation of the device relied on the passive hydrodynamic interaction of swimming cells of *E. coli* with the fluid, and walls of the channels, in the device; because swimming bacteria are self-propelled it was not necessary to use external pumping—or any other active, external elements—to drive cells through the device. By coupling three sorting junctions together in a single device, we were able to isolate a fraction of short cells in which over 90% of cells had lengths that were below the average length of cells entering the device. We estimate that each cell took approximately 4.7 min—or 8% of the 60 min generation time[3] of K12-derived *E. coli* at 25 °C—to swim through the three sorting junctions.

Directing *E. coli* with ratcheting microchannels

When motile cells of *E. coli* swim in an unrestricted, liquid environment, they execute three-dimensional random walks.[4] In the absence of any attractant or repellant cues, the average displacement with time of a population of *E. coli* swimming in a stationary fluid is zero. In order to facilitate the development of microdevices for studying bacteria, it is desirable to develop methods for controlling the direction of motion of a swimming bacterium. Such methods would be useful for directing bacteria through devices and for effecting relatively large-scale, directed displacements of populations of cells.

A small number of researchers have developed techniques for producing unidirectional movement in microorganisms. Uyeda and coworkers have demonstrated the use of microfabricated tracks to guide the motion of the teardrop-shaped, gliding bacterium *Mycoplasma mobile.*[5] The mechanism for unidirectional guidance in this method was specific to the gliding motility of *M. mobile.* Austin and coworkers developed a one-way gate for swimming *E. coli.*[6] The gate consists of a wall of evenly spaced V-shaped features. Because of the tendency of *E. coli* to swim along walls,[2] cells are funneled though the wall when swimming in one direction, but are diverted away from the wall when swimming in the opposite direction; in this manner, the gate was able to direct swimming *E. coli* from one chamber to another. Based on the same principle—the tendency of *E. coli* to swim along the walls of microfluidic channels—we have developed ratcheting microchannels that direct cells along a defined path, and thus produce a stream of *E. coli* moving in a single direction.

Fractionating *E. coli* by length

The bacterium *E. coli* is a rod-shaped organism, which grows by doubling its length while maintaining a constant width, and then divides symmetrically at its midpoint to reproduce. The resulting daughter cells are one-half the length of the parent cell. As each daughter cell ages and grows, the cycle of lengthening and division repeats.[7–9] Because the length of a bacterium is a measure of its progression through its growth cycle, a method for separating short cells from a population of bacterial cells would

[a]*Department of Chemistry and Chemical Biology, Harvard University, Cambridge, MA, 02138, USA*
[b]*Division of Engineering and Applied Sciences, Harvard University, Cambridge, MA, 02138, USA*
[c]*Rowland Institute at Harvard, Cambridge, MA, 02142, USA*

be useful for creating synchronized cultures of cells—cultures in which all the cells are at a similar point in the cell cycle, and thus have similar lengths. A technology of this kind would be useful to microbiologists wishing to examine the variation of gene and protein expression throughout the cell cycle,[10,11] or the variation in the time required to pass through the cell cycle.[12,13]

Several techniques exist in the literature for producing synchronous cultures of bacterial cells by isolating the youngest, and smallest, cells in a population. In one approach—growth cycle arrest—mutations and/or chemical treatment cause cells to accumulate at a specific stage of development (for example, initiation of DNA replication). Cells can then be released from arrest synchronously.[14] A drawback to this method is the physiological stress it places on bacteria; growth cycle arrest, by its nature, disrupts the natural physiological state of a bacterium. In the so-called 'baby machine'[15] and related techniques,[16] cells from an asynchronous population are affixed to a solid, porous support (a membrane or a column). As growth media flows through the solid support, cells that are attached to the support divide, forming one daughter cell that remains attached, and one daughter cell that is swept into a collector by the flowing liquid. In another method,[17] an asynchronous population of bacteria is spun in a centrifuge tube in which the centrifugal sedimentation of cells is counteracted by an upward stream of liquid media. The flow rate of the media can be adjusted such that the shortest cells are carried out of the centrifuge chamber while longer cells remain in the sedimentation field.

A potential drawback to these established methods for separating cells is the mechanical stress that they place on bacteria. In the baby machine and the centrifugation/flow technique, bacteria—in particular, bacteria that are attached to a solid support—could be subject to shear stress from the flow of liquid. Because shear stress may damage the fragile flagella of motile bacteria, methods that use external flow should be avoided, if possible, in experiments involving populations of swimming (and therefore flagellated) bacteria. In addition, in a popular variation of the baby machine—the 'baby-cell column'[16]—cells are affixed to a solid support *via* truncated, 'sticky' flagella. This method is not ideal for use with motile cells of *E. coli* because of the necessary disruption to normal flagellar synthesis.

We believed it would be useful to develop a technique for manipulating and sorting cultures of motile cells of *E. coli* that minimized (or eliminated) chemical and physical stress on the cells; such a method would be complementary to the methods described above for generating synchronous cultures. In addition, we wanted to develop a *microfabricated* device, for the production of semi-synchronous cultures in lab-on-a-chip bioanalytical devices. We present a microfluidic device for (i) manipulating the motion of swimming *E. coli*, and (ii) fractionating cells of swimming *E. coli* by length. The device takes advantage of the hydrodynamic interactions between swimming cells and the walls of the microchannel in order to guide cells unidirectionally through the device and to separate the shortest cells from the population. We illustrate a capability for linear integration of the tools that we developed—ratchets and sorters—by coupling multiple sorting junctions; this coupling increased the sorting ability of the system.

Results and discussion

Fabrication of composite agar/PDMS devices

We have previously used PDMS microchannels conformally sealed to an agar surface to examine swarming cells of *E. coli* that were migrating near the agar surface.[2] In these composite agar/PDMS devices, the floor of the microchannels is agar, and the ceiling and sidewalls are PDMS. Here, we used composite agar/PDMS microchannels to manipulate the motion of swimming cells of *E. coli* grown in liquid culture. Fig. 1 shows the assembly of a composite agar/PDMS device. Using standard soft lithographic procedures,[1] we fabricated a thin (1 mm) film of PDMS embossed with microchannels. Immediately prior to placing the PDMS film in conformal contact with an agar surface, we exposed the film to an oxidizing air plasma, which rendered the surface of the film hydrophilic. Upon contact of the hydrophilic film with the agar, liquid from the agar hydrogel filled the embossed channels of the film. A 2 mm hole through the PDMS film provided access to the microchannels.

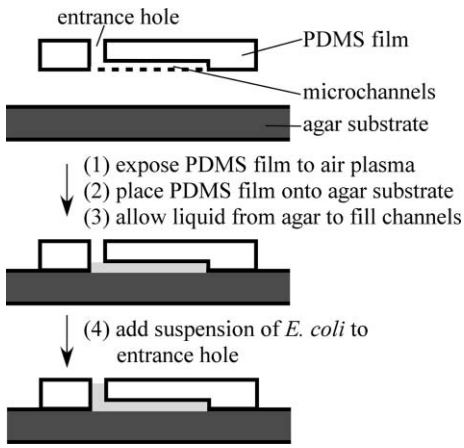

Fig. 1 Assembly of composite agar/PDMS devices. A film of PDMS, embossed with microchannels, was fabricated using soft lithography. The film was exposed to an oxidizing air plasma and placed in conformal contact with an agar substrate. Because of the hydrophilicity of the oxidized PDMS film, liquid from the agar filled the microchannels of the PDMS film upon contact of the PDMS with the agar. To introduce cells into the device, we added a 2–5 μL suspension of *E. coli* (10^9 cells mL^{-1}) at the entrance of the device.

Design of ratcheting microchannels

In order to guide cells unidirectionally through the device, we developed ratcheting microchannels for *E. coli.* Fig. 2(A) shows a single ratchet; multiple ratchets in succession created a ratcheting microchannel. We have previously demonstrated that when cells of *E. coli* are confined in shallow channels (1.5 μm tall) with agar floors and PDMS sidewalls and ceilings, cells preferentially swim closer to the bottom agar surface and swim on the right-hand side of the microchannel.[2] Our ratcheting channels take advantage of this tendency for cells to swim along the right-hand side of a microchannel; the arrowhead shape of the channels ensures that any cell swimming in the 'wrong' direction is quickly redirected. Both Hiratsuka *et al.* and Jia *et al.* have used similar arrowhead patterns to direct

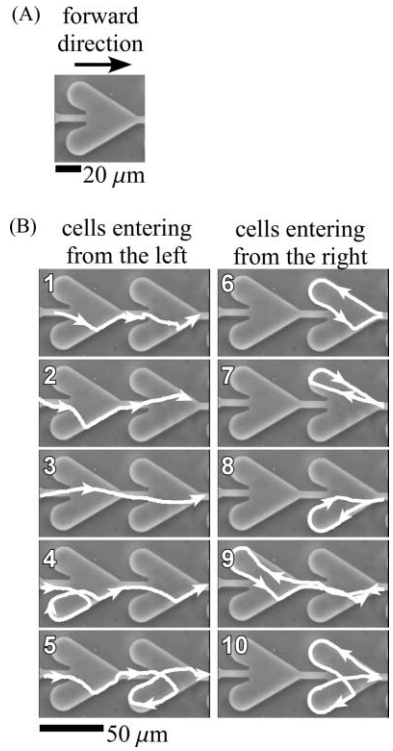

Fig. 2 Directing cell movement in bacterial ratchets. The ability of bacterial ratchets to direct the motion of motile cells of *E. coli* was tested in composite agar/PDMS channels. (a) A single ratchet. The arrow indicates the direction in which the ratchet guided cells. (b) Representative trajectories of cells swimming in the bacterial ratchets. Trajectories 1–5 show the paths that cells followed as they moved through the microchannel in the forward direction (from left to right). Trajectories 6–10 show the paths that motile cells took as they were redirected by the ratcheting microchannel.

the movement of microtubules on kinesin tracks[18,19] (the linear tracks of kinesin within microchannels produced bidirectional motion of microtubules; the arrowhead patterns forced the microtubules to move in one direction only).

The design of the ratcheting microchannels was such that the microchannel permitted the continuous movement of cells in one direction, and redirected cells that were traveling in the opposite direction. We monitored the motion of cells of *E. coli* in a microchannel composed of 500 sequential ratchets. The device was constructed of agar and PDMS, as shown in Fig. 1. Fig. 2(B) shows samples of the trajectories of cells swimming in the bacterial ratchets. In trajectories 1–5, cells entered from the left and continued to swim through the ratcheting microchannel in the forward direction. (We define the "forward direction" to be from left to right in Fig. 2.) In trajectories 6–10, the ratcheting microchannel redirected cells that entered from the right. If a cell tumbled at any location within the channel, it was ultimately redirected forward in the channel. Thus, the ratchets produced unidirectional movement of cells in composite agar/PDMS microchannels.

We tested the capability of the ratchets to redirect cells by observing (i) the number of cells that entered a single ratchet from the right (in Fig. 2) and exited to the left from that ratchet (N_{RL}), and (ii) the number of cells that entered the ratchet from the right and exited to the right (N_{RR}). Eqn (1) defines the redirecting efficiency of the bacterial ratchets, η.

$$\eta = \frac{N_{RR}}{N_{RR} + N_{RL}} 100\% \quad (1)$$

A single ratchet (Fig. 2(A)) redirected $\eta = 91\%$ of cells that entered that ratchet from the wrong direction ($N_{RR} + N_{RL} =$ 395 cells). The redirecting efficiency of two sequential ratchets increased to $\eta = 98\%$ ($N_{RR} + N_{RL} = 395$ cells). A serial sequence of three ratchets had an aggregated redirecting efficiency that approached 100% ($N_{RR} + N_{RL} = 395$ cells). We also calculated the average rate of displacement of a cell moving through the ratcheting microchannels by monitoring the movement of the cells through three sequential ratchets, and dividing the distance along the central axis of the three ratchets (105 μm) by the average time that it took the cells to pass through the three ratchets. The average rate of displacement of the cells was (32 ± 9) μm s^{-1}. Despite the fact that the cells occasionally tumbled within the ratchets, this rate of displacement is similar to the velocity of a cell swimming (without tumbling) along the right-hand side of a smooth-walled composite agar/PDMS microchannel,[2] (31 ± 3) μm s^{-1}. The ratcheting microchannels thus produced rapid transport of cells from one point to another.

Trapping and concentrating cells with bacterial ratchets

The unidirectional movement of cells in bacterial ratchets enabled us to trap and concentrate bacterial cells in microchannels. When the ratcheting channels led to a dead end, cells swam to the end of the channel and became trapped. In the sorting device, these bacterial traps were useful, because they directed sorted cells away from the sorting junctions, and thus prevented those cells from returning to the junction and interfering with the sorting process. Fig. 3 shows a series of fluorescence micrographs, which show green fluorescent protein-labeled (GFP-labeled) cells becoming trapped at the end of a ratcheting microchannel over a period of 8 minutes. Over this period, more and more cells accumulated at the end of the channel, such that the final ratchets in the channel became packed with cells. These filled ratchets appear bright in Fig. 3 because the bacterial cells were labeled with GFP.

Design of the sorting junction

In addition to the ratcheting microchannels, a second element of the sorting device was the sorting junction itself. The design of the sorting junction was based on the observation that when an *E. coli* cell swims close to a surface, it swims in a clockwise, circular path along the surface.[20–22] This circular trajectory is due to the chiral, rotatory mechanism by which the bacterium swims: *E. coli* swims using two to six rotary motors, which are embedded in its cell wall and are attached to external rigid flagellar filaments.[23,24] When all the motors turn counter-clockwise (CCW) (when viewed from behind), the flagella bundle together and propel the cell body forward in a "run". The frequency of rotation of the flagellar bundle is ~100 Hz.[25] When one or more of the motors switches to clockwise (CW) rotation, the flagella unbundle and the body of the cell moves erratically in a "tumble".[26] To balance the torque that the CCW rotation of the

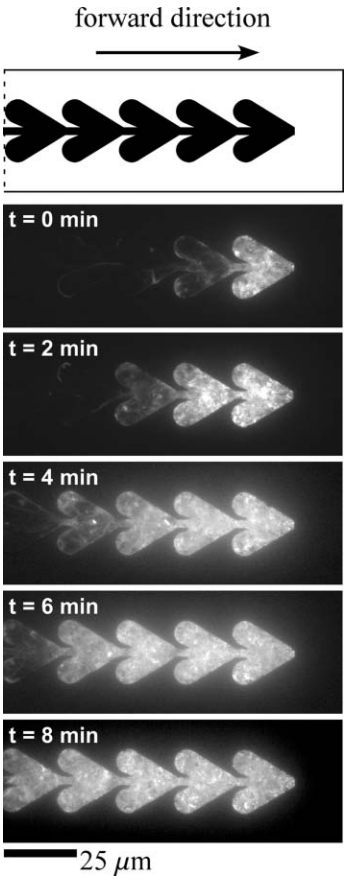

Fig. 3 Time-lapse images of fluorescent *E. coli* cells being trapped and concentrated in bacterial ratchets. We examined GFP-labeled *E. coli* cells as they entered a ratcheting microchannel with a dead end. The arrow indicates the direction in which the ratchet guided cells. The top panel shows a schematic illustration of the geometry of the channel. The bacterial ratchets directed the cells towards the end of the channel; because there was a dead end, the cells were trapped. In the first image of the time series—at $t = 0$ min—cells were already trapped in the end of the channel. The ratchets at the end of the channel lit up with fluorescent signal as they became filled with GFP-labeled cells.

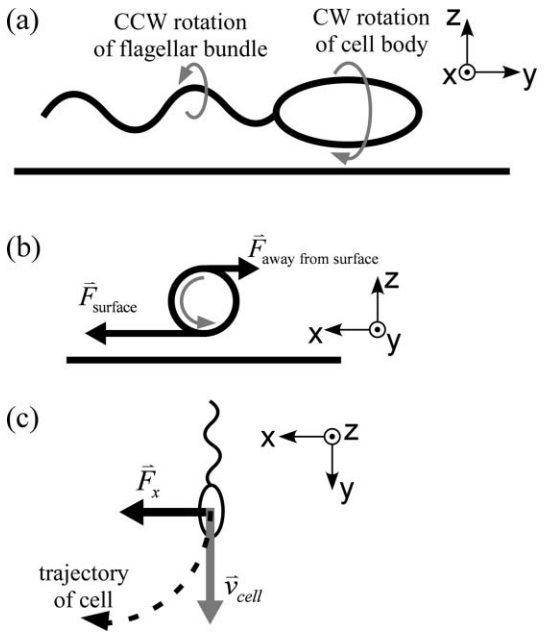

Fig. 4 Motile cells of *E. coli* swim in circles at surfaces. (a) Side view. To propel itself forward, a cell of *E. coli* rotates its flagellar bundle counter-clockwise (when viewed from behind). This counter-clockwise rotation is balanced by clockwise rotation of the body of the cell. The gray arrows indicate the direction of rotation of the body of the cell and its flagellar bundle. (b) Front view. When the bacterium swims near a surface, there is increased viscous drag (due to the rotation of the body of the cell) on the side of the cell that is closest to the surface. As a result of this asymmetric drag, there is a net force on the cell, $\vec{F}_x$. (c) Top view. As a result of $\vec{F}_x$, a cell swimming at velocity $\vec{v}_{\text{cell}}$ near a planar surface will swim in a clockwise (when viewed from above), circular trajectory (indicated by the dashed line).

flagellar bundle creates during a run, the body of the cell rotates in the opposite direction (Fig. 4(a)), at ~10 Hz.[25] As the body of the cell rotates in a liquid medium, the rotation is opposed by hydrodynamic drag. When a cell swims close to a planar surface, the magnitude of the hydrodynamic drag is higher on the side of the cell that is closer to the surface (compared to the side of the cell that is further from the surface). Because of this imbalance of forces, the cell experiences a non-zero net force, labeled $\vec{F}_x$ in Fig. 4(b). As a combined result of this force ($\vec{F}_x$) and the forward swimming motion of the cell itself, a cell swimming near a surface swims in a clockwise (when viewed from above), circular path (Fig. 4(c)).[23,24,27,28]

We have previously observed that there is a weak correlation between the radius of curvature of the circular trajectory of a cell and the length of that cell;[25] therefore, the radius of curvature of the trajectory of a cell should correspond to the progression of the cell through its life cycle. The sorting junction that we have developed to exploit this correlation is essentially a curved microchannel with multiple outlets (Fig. 5(a)): cells swimming along the right-hand side of the microchannel leading up to the junction are sorted into one of three outlet channels (labeled channels 1–3 in Fig. 5(a)). We anticipated a tendency for a greater number of shorter cells than longer cells to follow the sharp radius of curvature of the sorting junction. Because we were interested in isolating the shortest cells from the population, we were primarily interested in the cells that were able to follow the curvature of the sorting junction completely, *i.e.* the cells that exited the junction through channel 1 in Fig. 5(a). Cells that were less able to follow the curvature of the sorting junction (and were, we expected, longer) exited the junction through channel 2 or 3. Cells that entered the sorting junction swimming either in the center of, or along the left-hand side of, the entrance microchannel would exit the junction through channels 4 or 5, respectively. The curved arrow in Fig. 5(a) shows the expected path for short cells swimming through the junction. We designed the sorting junction to sort only those cells swimming on the right-hand side of the channel leading up to the junction because of our previous observation that in composite agar/PDMS microchannels, the majority of cells (75%) swim on the right-hand side of the microchannel (when viewed through the PDMS).[2]

Fractionating cells of *E. coli* by length

The design of the complete sorting device (Fig. 5) incorporated both bacterial ratchets and sorting junctions. In order to improve

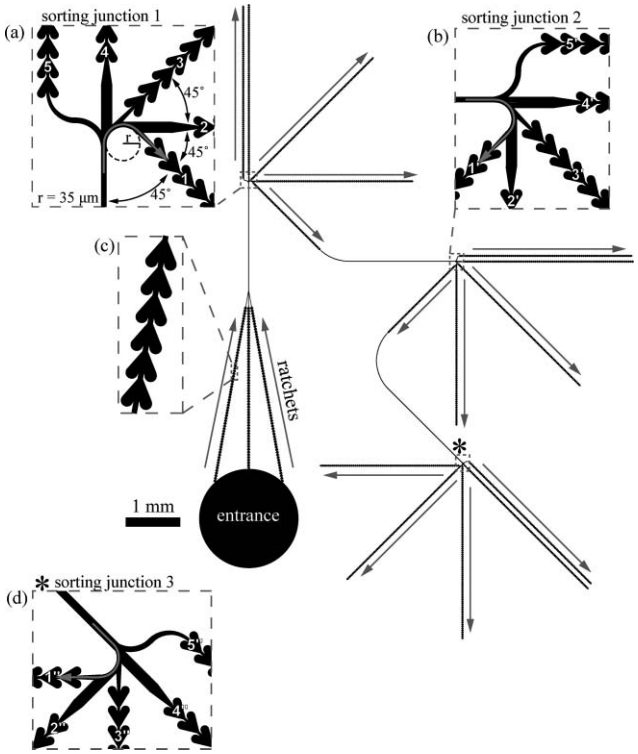

Fig. 5 The microfluidic sorting device. A combination of ratcheting microchannels and sorting junctions formed the sorting device. The straight gray arrows indicate the presence of ratcheting microchannels (elsewhere in the device, the channels have smooth walls). Three ratcheting microchannels lead from the entrance of the device to sorting junction 1. Cells entering sorting junction 1 were sorted into one of five outlet channels, labeled 1–5. Channel 1 from sorting junction 1 was coupled to a second sorting junction (sorting junction 2). Channel 1′ from sorting junction 2 was coupled to a third sorting junction (sorting junction 3). The junctions were coupled such that ratcheting microchannels guided the shortest cells from one sorting junction to the next sorting junction. The radius of curvature of each sorting junction was $r = 35$ μm. The curved arrows indicate the path of cells that were able to follow the sharp radius of curvature of the sorting junctions (the shortest cells). The inset diagrams show expanded views of (a) sorting junction 1, (b) sorting junction 2, (c) ratcheting microchannels, and (d) sorting junction 3 (the location of sorting junction 3 in the device is indicated by *).

the sorting ability of the device, the design coupled three sorting junctions together using ratcheting microchannels. We introduced cells into the device by placing a 2 μL suspension (10^9 cells mL^{-1}) of cells at the entrance of the device. From the entrance, three ratcheting microchannels directed cells towards the first sorting junction (sorting junction 1, Fig. 5(a)). The presence of three ratcheting channels increased the number of cells entering the device.

At sorting junction 1, the device sorted cells into the five different downstream channels (as described above in Section 2.4). Sorting junctions 2 and 3 (Fig. 5(b),(d)) were identical in geometry to sorting junction 1. The outlet channels for sorting junction 2 are labeled 1′–5′; the outlet channels for sorting junction 3 are labeled 1″–5″. Cells that were able to follow the curvature of sorting junction 1 completely (indicated by the curved arrow in Fig. 5(a)) were guided by a ratcheting microchannel to a second sorting junction (Fig. 5b). Cells that were able to follow the curvature of sorting junction 2 completely (indicated by the curved arrow in Fig. 5(b)) were guided to a third sorting junction (Fig. 5(d)). Cells that were able to follow the curvature of sorting junction 3 completely (indicated by the curved arrow in Fig. 5(d)) were trapped in the ratcheting microchannels that extended from outlet channel 1″ in sorting junction 3.

The distance along the axis of the path leading from sorting junction 1 to sorting junction 3 was approximately 9000 μm. Because the average rate of displacement of cells through the ratcheting microchannels was (32 ± 9) μm s^{-1}, we estimate that it would take approximately 4.7 min for a cell to travel from sorting junction 1 to sorting junction 3. This value (4.7 min) is roughly 8% of 60 min, the generation time for K12-derived *E. coli* at 25 °C.[3] It would be possible to reduce the overall distance that the cells must travel by shortening the regions of the device that contain ratcheting microchannels. It is not advisable, however, to eliminate any of the ratcheting regions from the design completely because the ratchets ensure that cells travel through the device unidirectionally.

Analysis of the lengths of fractionated cells

Using phase-contrast video microscopy, we collected movies of cells entering the device, and swimming through sorting junctions 1, 2 and 3. From these movies, we measured the lengths of the cells. Fig. 6 shows the distributions of lengths for (i) cells entering the device (Fig. 6(A)), (ii) cells exiting sorting junction 1 *via* channel 1 (Fig. 6(B)), (iii) cells exiting sorting junction 2 *via* channel 1′ (Fig. 6(C)), and (iv) cells exiting sorting junction 3 *via* channel 1″ (Fig. 6(D)). Cells exiting sorting junctions 1, 2, and 3 *via* channels 1, 1′, and 1″ represented the cells that were best able to follow the radius of curvature of the sorting junctions. As Fig. 6 shows, the average length of the cells, $\bar{x}$, decreased from 3.8 μm (Coefficient of Variation, CV: 21%) at the entrance, to 3.4 μm (CV: 16%) after one stage of sorting, to 3.2 μm (CV: 19%) after two stages of sorting, and, finally, to 3.0 μm (CV: 19%) after three stages of sorting. The median length of the cells decreased from 3.7 μm at the entrance, to 3.3 μm after one stage of sorting, to 3.1 μm after two stages of sorting, and, finally, to 3.0 μm after three stages of sorting. It is evident from Fig. 6 that successive stages of sorting resulted in successive decreases in the average length, and median length, of the population of cells; this observation suggests that the incorporation of additional sorting junctions into the device could further improve the ability of the device to isolate short cells. After three stages of sorting, the device had isolated a population enriched in short cells: within this isolated fraction (Fig. 6D), more than 90% of the cells were shorter than the mean length of cells entering the device.

Three principal factors influenced the sorting ability of the device. First, the sorting process was defined by the hydrodynamic interaction of the swimming cells with the sorting junction. This interaction depended on the shape of the microchannels and the relevant properties of the each cell—including the size of the body, the size of the flagellar bundle, the swimming velocity, and the rate of tumbling. Without a complete understanding of the sorting mechanism, it is difficult to speculate on the relative contributions of these properties. Second, because of their small size, bacteria are subject to translational and rotational

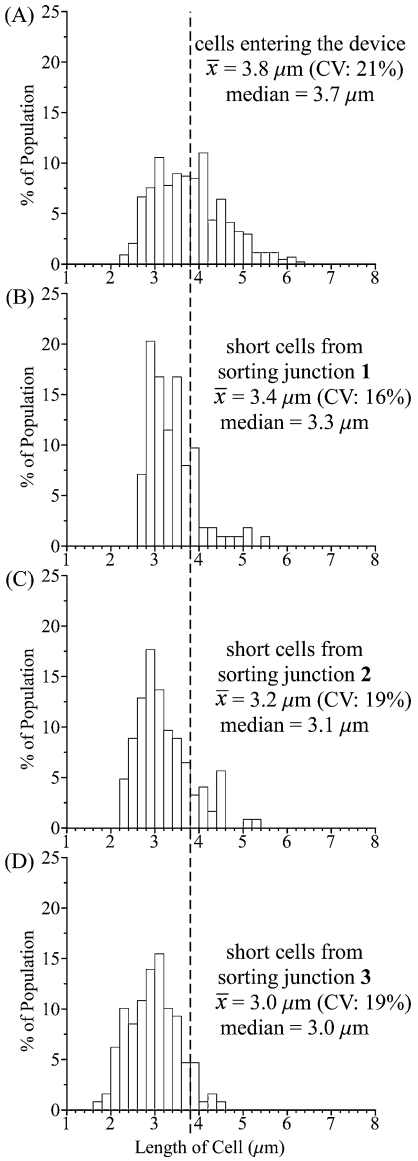

Fig. 6 Isolating short cells with the sorting device. Distributions of length for (A) cells entering the device (430 cells), (B) cells exiting sorting junction 1 *via* channel 1 (112 cells), (C) cells exiting sorting junction 2 *via* channel 1′ (123 cells), and (D) cells exiting sorting junction 3 *via* channel 1″ (128 cells). The dashed line indicated the mean length of cells entering the device (3.8 μm).

diffusion, which could have disrupted the trajectories of sorted cells and produced sorting errors. Third, imperfections in the fabrication of the device (for example, a rough spot on the wall of the channel) could have also produced errors in sorting.

Conclusions

We have developed microfabricated tools for manipulating the motion of motile cells of *E. coli*: bacterial ratchets, which force cells to swim unidirectionally in microchannels, and sorting junctions, which enable the separation and isolation of the shortest—and, we assume, youngest—cells from a population. Because these tools rely on the hydrodynamic interaction between a swimming cell and the geometry of the microchannel, the device requires no external pumping or flow; instead, motile cells propel themselves through the device. By combining ratcheting microchannels and three sorting junctions, we have designed a device that isolates a fraction of short, motile cells and does not inflict chemical and physical stress on the cells. Because the device isolates short cells from the population, we believe it would be possible to use this device to generate nearly synchronous populations of motile bacteria. This capability would be useful for studying the variation in gene and protein expression during the cell cycle[13] and how these processes relate to motility.[10,11] In addition to *E. coli*, it may be possible to use the device to sort other types of bacteria that swim using the rotation of helical flagellar filaments, such as *Vibrio*, *Pseudomonas*, or *Salmonella.*

The ratcheting microchannels were critical for the operation of the device; without unidirectional guidance, the system would not have worked. The bacterial ratchets represent a generically useful tool for the design on lab-on-chip devices for motile bacteria. In addition to the unidirectional guidance of swimming cells, the ratcheting microchannels could be used for separating motile cells from non-motile cells, or separating live motile cells from dead cells. It may thus be possible to use the ratchets to isolate motile bacteria from the environment. Because the ratchets can cause the accumulation of cells at high concentration at the end of a channel (as in Fig. 3), the ratcheting microchannels may also be useful for studying bacterial phenomena that depend on the concentration of a population, such as quorum sensing.

Because ratcheting microchannels can control the direction of movement of swimming cells along any arbitrary path, the ratchets could be valuable for the construction of devices in which cells of *E. coli* serve as microscale actuators and transporters. Previous studies have demonstrated that several types of biological materials—including both purified motor proteins[29–34] and intact cells[5,35,36]—have the potential to serve as driving units in micro-mechanical devices. Within the ratchets, the rate of displacement of cells along the axis of the channel is as fast as it would be for a cell swimming along a smooth-walled channel without tumbling.[2] The rate of displacement of cells within the ratchets is likely to be higher than the rate of displacement of cells in the 'one-way gate' developed by Austin and coworkers[6] because the ratchets constantly direct (and redirect) cells towards the desired direction, while the one-way gate directs cells from one large (200 μm) chamber to another—within these open chambers, the motion of the cells is not directed.

Experimental section

Growth of bacterial cells

For this work, we used *E. coli* strain AW405,[37] a wild-type, K12-derived strain that possesses all chemotaxis genes. Media components were purchased from Difco or Sigma unless otherwise noted. Saturated *E. coli* cultures were grown aerobically for 16 h at 32 °C in tryptone broth (TB, 1% tryptone and 0.5% NaCl) in a rotary shaker (200 rpm). Motile *E. coli* cultures were obtained by diluting the saturated culture (50 μL) into fresh TB (5 mL). These cells were grown to mid-log phase in 15 mL, sterile

polypropylene tubes at 32 °C in a rotary shaker (200 rpm) for 3.5 h. Cells were washed from growth media into motility buffer[38] (10 mM potassium phosphate, 76 mM NaCl, 0.1 mM Na-EDTA, pH 7.0) containing Pluronic surfactant (0.01% Pluronic F-68) by centrifuging the cells at 2000 × *g* for 10 min, pouring off the supernatant liquid, and resuspending the pelleted cells in motility buffer (5 mL). This centrifugation/resuspension process was repeated three times in total.

Preparation of GFP-expressing cells

We prepared a green fluorescent protein (GFP) producing strain of *E. coli* by transforming cells of *E. coli* strain AW405 with pEGFP (BD Biosciences) using a solution-phase protocol developed by Chung and coworkers.[39] Motile, fluorescent cells were prepared by first growing an overnight culture to saturation in TB containing 100 μg mL^{-1} ampicillin on a rotary shaker (150 rpm) at 32 °C. The saturated culture was then diluted 1 : 100 into fresh TB containing 100 μg mL^{-1} ampicillin and 0.1 mM isopropyl-1-thio-β-D-galactosidase (IPTG) and grown on a rotary shaker (150 rpm) at 32 °C for 3.5 h. Cells were washed into motility buffer containing 0.01% Pluronic F-68 surfactant, 100 μg mL^{-1} ampicillin, and 0.1 mM IPTG using centrifugation and resuspension, as described above.

Fabrication of silicon masters

Using standard photolithographic procedures,[40] we prepared silicon masters—features of SU-8 photoresist (Microchem Corp., Newton, MA) in relief on a silicon wafer (Silicon Sense, Inc., Nashua, NH). For all devices in this study, the height of the features on the master was approximately 1.5 μm. The silicon masters served as templates for replica molding devices in poly(dimethyl siloxane) (PDMS).[40] To prevent PDMS from adhering to the master during the molding process, we silanized the master with tridecafluoro(1,1,2,2-tetrahydrooctyl) trichlorosilane (Gelest, Inc., Philadelphia, PA) prior to molding.

Preparation of composite agar/PDMS microchannels

To mold PDMS microchannels from a master, we poured PDMS pre-polymer (Dow Corning Sylgard 184, Dow Corning Corp., Corning, NY) onto the surface of the master and cured the PDMS at 60 °C for at least 3 h. The resulting PDMS film was approximately 1 mm thick. We peeled the flexible film from the master and punched a 2 mm entrance hole using a biopsy punch (Shoney Scientific). To form the composite agar/PDMS microchannels, we exposed the embossed side of the PDMS film to an oxidizing air plasma for 1 min at 1 Torr immediately before use, and subsequently placed the hydrophilic film in conformal contact with a surface of motility agar (motility buffer with 1% Bacto™ agar) containing 0.01% Pluronic F-68 surfactant. We added L-serine (1 mM) to the motility agar during sorter experiments to increase the average run time of wild-type *E. coli* cells.[41] To load cells into a composite agar/PDMS device, we pipetted a concentrated suspension of *E. coli* cells (2–5 μL, 10^9 cells mL^{-1}) in motility buffer into the entrance. Experiments were performed at room temperature.

Image acquisition and data analysis

We monitored cells within the composite agar/PDMS devices using fluorescence microscopy or phase-contrast video microscopy. Fluorescence microscopy images were acquired using an upright Leica DMRX microscope equipped with a 20× APO objective, a 1.3× camera relay lens, a monochrome CCD camera (Hamamatsu Orca-ER) and Metamorph software. Phase-contrast video microscope images were acquired using an upright Nikon E400 microscope equipped with a 20× Nikon phase-contrast objective, a 2.5× camera relay lens, and a monochrome CCD camera (Marshall Electronics V1070) connected to a digital video recorder (Sony GV-D1000), which collected images at 30 frames per second. Video was captured using Adobe Premiere and analyzed using ImageJ (available for download at http://rsbweb.nih.gov/ij/) or MATLAB (The MathWorks, Inc.). In ImageJ, trajectories of cells in the ratchets were found by tracking the midpoint of the cells in each video frame.

To analyze the lengths of cells in the sorting device, we imported digital video segments, 30 s in length, of cells swimming in the device into MATLAB. Each frame of the video was thresholded to produce a binary image of white objects on a black background. Objects less than 0.6 μm^2 were assumed to be background, and were removed from the analysis. Using MATLAB, we constructed algorithms to give unique labels to every cell in each frame and to measure the relevant properties of each cell (the centroid position, and the major and minor axes of an ellipse that had the same normalized second central moment as the cell in the image). The centroid of each cell was tracked from frame to frame. The centroid position of each cell was assumed to move less than 2 μm per frame (1/30 s). In the ambiguous cases in which (i) more than one cell was within 2 μm of a single cell in the previous frame, or (ii) no cells were within 2 μm of a cell in the previous frame, the program truncated the current trajectory and began tracking a new cell. Cells with trajectories less than 5 frames long were not used in the analysis.

Acknowledgements

We thank H. A. Stone, E. Lauga, N. Darnton, and R. Castillejos for helpful discussions. This research was supported by the DOE (DE-FG02-OOER45852). W.R.D. acknowledges an NSF-IGERT Biomechanics Training Grant (DGE-0221682). S.E.H. acknowledges a NDSEG Fellowship. M.M. acknowledges a postdoctoral fellowship from the Novartis Foundation.

References

1 Y. Xia and G. M. Whitesides, *Angew. Chem., Int. Ed.*, 1998, **37**, 550–575.
2 W. R. DiLuzio, L. Turner, M. Mayer, P. Garstecki, D. B. Weibel, H. C. Berg and G. M. Whitesides, *Nature*, 2005, **435**, 1271–1274.
3 C. Pin and J. Baranyi, *Appl. Environ. Microbiol.*, 2006, **72**, 2163–2169.
4 H. C. Berg, *Random Walks in Biology*, Princeton University Press, Princeton, NJ, 1993.
5 Y. Hiratsuka, M. Miyata and T. Q. Uyeda, *Biochem. Biophys. Res. Commun.*, 2005, **331**, 318–324.
6 P. Galajda, J. Keymer, P. Chaikin and R. Austin, *J. Bacteriol.*, 2007, **189**, 8704–8707.
7 T. Nystrom, *Curr. Opin. Microbiol.*, 2002, **5**, 596–601.

8 E. J. Stewart, R. Madden, G. Paul and F. Taddei, *PLoS Biol.*, 2005, **3**, 1–6.
9 *Escherichia coli and Salmonella: Cellular and Molecular Biology*, 2nd edn., ed. F. C. Neidhardt and R. Curtiss, ASM Press, Washington, DC, 1996.
10 S. I. Aizawa and T. Kubori, *Genes Cells*, 1998, **3**, 625–634.
11 B. M. Pruss and P. Matsumura, *J. Bacteriol.*, 1997, **179**, 5602–5604.
12 F. Kepes, *FEMS Microbiol. Rev.*, 1986, **32**, 225–246.
13 A. L. Koch, *Crit. Rev. Microbiol.*, 2002, **28**, 61–77.
14 P. L. Carl, *Mol. Gen. Genet.*, 1970, **109**, 107–122.
15 C. E. Helmstetter and D. J. Cummings, *Proc. Natl. Acad. Sci. U. S. A.*, 1963, **50**, 767–774.
16 D. Bates, J. Epstein, E. Boye, K. Fahrner, H. Berg and N. Kleckner, *Mol. Microbiol.*, 2005, **57**, 380–391.
17 C. G. Figdor, A. J. M. Olijhoek, S. Klencke, N. Nanninga and W. S. Bont, *FEMS Microbiol. Lett.*, 1981, **10**, 349–352.
18 Y. Hiratsuka, T. Tada, K. Oiwa, T. Kanayama and T. Q. Uyeda, *Biophys. J.*, 2001, **81**, 1555–1561.
19 L. Jia, S. G. Moorjani, T. N. Jackson and W. O. Hancock, *Biomed. Microdevices*, 2004, **6**, 67–74.
20 H. C. Berg and L. Turner, *Biophys. J.*, 1990, **58**, 919–930.
21 P. D. Frymier, R. M. Ford, H. C. Berg and P. T. Cummings, *Proc. Natl. Acad. Sci. U. S. A.*, 1995, **92**, 6195–6199.
22 M. A. S. Vigeant and R. M. Ford, *Appl. Environ. Microbiol.*, 1997, **63**, 3474–3479.
23 H. C. Berg and R. A. Anderson, *Nature*, 1973, **245**, 380–382.
24 H. C. Berg, *Annu. Rev. Biochem.*, 2003, **72**, 19–54.
25 E. Lauga, W. R. DiLuzio, G. M. Whitesides and H. A. Stone, *Biophys. J.*, 2006, **90**, 400–412.
26 L. Turner, W. S. Ryu and H. C. Berg, *J. Bacteriol.*, 2000, **182**, 2793–2801.
27 M. Meister, G. Lowe and H. C. Berg, *Cell*, 1987, **49**, 643–650.
28 M. Ramia, D. L. Tullock and N. Phanthien, *Biophys. J.*, 1993, **65**, 755–778.
29 K. J. Bohm, R. Stracke, P. Muhlig and E. Unger, *Nanotechnology*, 2001, **12**, 238–244.
30 H. Hess, J. Clemmens, D. Qin, J. Howard and V. Vogel, *Nano Lett.*, 2001, **1**, 235–239.
31 S. Diez, C. Reuther, C. Dinu, R. Seidel, M. Mertig, W. Pompe and J. Howard, *Nano Lett.*, 2003, **3**, 1251–1254.
32 G. D. Bachand, S. B. Rivera, A. K. Boal, J. Gaudioso, J. Liu and B. C. Bunker, *Nano Lett.*, 2004, **4**, 817–821.
33 R. Yokokawa, S. Takeuchi, T. Kon, M. Nishiura, K. Sutoh and H. Fujita, *Nano Lett.*, 2004, **4**, 2265–2270.
34 R. Yokokawa, Y. Yoshida, S. Takeuchi, T. Kon and H. Fujita, *Nanotechnology*, 2006, **17**, 289–294.
35 N. Darnton, L. Turner, K. Breuer and H. C. Berg, *Biophys. J.*, 2004, **86**, 1863–1870.
36 D. B. Weibel, P. Garstecki, D. Ryan, W. R. DiLuzio, M. Mayer, J. E. Seto and G. M. Whitesides, *Proc. Natl. Acad. Sci. U. S. A.*, 2005, **102**, 11963–11967.
37 J. B. Armstrong, J. Adler and M. M. Dahl, *J. Bacteriol.*, 1967, **93**, 390–398.
38 J. Adler and B. Templeton, *J. Gen. Microbiol.*, 1967, **46**, 175–184.
39 C. T. Chung, S. L. Niemela and R. H. Miller, *Proc. Natl. Acad. Sci. U. S. A.*, 1989, **86**, 2172–2175.
40 S. K. Sia and G. M. Whitesides, *Electrophoresis*, 2003, **24**, 3563–3576.
41 H. C. Berg and D. A. Brown, *Nature*, 1972, **239**, 500–504.